# REVISTA MEXICANA DE CIENCIAS GEOLÓGICAS

Revista Mexicana de Ciencias Geológicas, v. 42, num. 3, December 2025, p. 160–169 ISSN-L 2007-2902 https://rmcg.unam.mx

Type: Original research





# An analysis of rheological models for lahar modelling with Iber

Marcos Sanz-Ramos<sup>1\*</sup>, Ernest Bladé<sup>1</sup>, Andrés Díez-Herrero<sup>2</sup>, Daniel Vázquez-Tarrío<sup>2</sup>, Julio Garrote<sup>3</sup>, Nieves Sánchez<sup>4</sup>, and Inés Galindo<sup>4</sup>

<sup>1</sup>Institut Flumen, Universitat Politècnica de Catalunya - BarcelonaTech (UPC) - Centre Internacional de Mètodes Numèrics en Enginyeria (CIMNE), Gran Capità s/n, 08034, Barcelona, Spain.

<sup>2</sup>Instituto Geológico y Minero de España (IGME, CSIC), Ríos Rosas 23, 28003, Madrid (Comunidad de Madrid), Spain.

<sup>3</sup>Dept. Geodinámica, Estratigrafía, y Paleontología, Facultad de Ciencias Geológicas, Universidad Complutense de Madrid (UCM), Calle José Antonio Nováis, 12. 28040, Madrid (Comunidad de Madrid), Spain.

<sup>4</sup>Instituto Geológico y Minero de España (IGME, CSIC), Unidad Territorial de Canarias, Spain.

# **E**DITORS:

Luigi A. Solari Lucia Capra

# How to cite:

Sanz-Ramos, M., Bladé, E., Díez-Herrero, A., Vázquez-Tarrío, D., Garrote, J., Sánchez, N., & Galindo, I. (2025). An analysis of rheological models for lahar modelling wi

th Iber. *Revista Mexicana de Ciencias Geológicas*, 42(3), 160–169. DOI: https://dx.doi.org/10.22201/igc.20072902e.2025.3.1882

Manuscript received: June 5, 2025 Corrected manuscript received: September 26, 2025 Manuscript accepted: October 13, 2025 Published online: December 1, 2025

# **C**OPYRIGHT

© 2025 The Author(s).

This is an open-access article published and distributed by the Universidad Nacional Autónoma de México under the terms of a <u>Creative Commons Attribution 4.0 International License (CC BY)</u> which permits unrestricted use, distribution, and reproduction in any medium, provided the original author and source are credited.





# **ABSTRACT**

Lahars are destructive volcanic debris flows, composed of water and pyroclastic material, capable of traveling long distances at high velocities. Modelling their dynamics is critical for hazard assessment and risk mitigation, yet it remains complex due to factors such as parameter uncertainty, limited calibration data, and variable terrain topography. Current modelling approaches range from empirical methods to advanced depth-averaged numerical simulations, where flow resistance is typically represented through rheological models. Common formulations include the Manning equation, Voellmy friction model, and Bingham plastic rheology, each capturing different aspects of non-Newtonian flow behaviour. This study evaluates the performance of several rheological models in reconstructing the 2001 lahar event at Popocatépetl volcano (Mexico) using the enhanced non-Newtonian module of the Iber hydrodynamic modelling tool (Iber-NNF). Results show that model choice significantly affects simulation accuracy. Manning-like models performed poorly, highlighting the limitations of velocity-dependent resistance terms in capturing static flow behaviour.

Keywords: non-Newtonian flows; Popocatépetl volcano; hazard assessment.

# **RESUMEN**

Los lahares son flujos destructivos ligados a áreas volcánicas, compuestos de agua y material piroclástico, capaces de recorrer largas distancias a altas velocidades. Simular su dinámica es crucial para la evaluación de peligros y la mitigación de riesgos; sin embargo, esto sigue siendo complejo debido a factores tales como la incertidumbre de los parámetros, la escasez de datos de calibración y la variabilidad topográfica del terreno. Los enfoques actuales para su evaluación abarcan desde métodos empíricos hasta simulaciones numéricas avanzadas promediadas en profundidad, donde la resistencia al flujo se representa típicamente mediante modelos reológicos. Las formulaciones comunes incluyen la ecuación de Manning, el modelo de fricción de Voellmy y la reología plástica de Bingham, cada una de las cuales captura diferentes aspectos del comportamiento del flujo no newtoniano. Este estudio evalúa el rendimiento de varios modelos reológicos en la reconstrucción del evento de lahar ocurrido en 2001 en el volcán Popocatépetl (México) utilizando el módulo no newtoniano mejorado

de la herramienta de modelado hidrodinámico Iber (Iber-NNF). Los resultados muestran que la elección del modelo afecta significativamente la precisión de la simulación. Los modelos tipo Manning tuvieron un rendimiento deficiente, lo que pone de relieve las limitaciones de los términos de resistencia dependiente de la velocidad para capturar el comportamiento estático del flujo.

Palabras clave: flujos no newtonianos; volcán Popocatépetl; gestión del riesgo.

#### INTRODUCTION

Lahars are a kind of debris flow that occur in volcanic settings, consisting of a mixture of volcanic fragments and water. These flows can be highly destructive due to their high velocity, large volume, and capacity to travel considerable distances downstream from the releasing area. Consequently, lahar modelling remains a significant challenge, while it is essential for hazard assessment, risk management, and the development of effective mitigation strategies (Huggel *et al.* 2003; Sheridan *et al.* 2004; Capra *et al.* 2004; Darnell *et al.* 2013; Caballero and Capra 2014; Woodhouse *et al.* 2016; Mead and Magill 2017; Guerrero *et al.* 2019).

Available approaches for lahar simulation range in complexity from simple empirical models (e.g., Schilling 2014) to advanced numerical simulation tools (e.g., Haddad et al. 2010). Currently, the most widely used method involves depth-averaged hydrodynamic numerical tools, which apply fundamental physical laws to simulate flow behaviour, incorporating resistance forces through rheological models.

A variety of rheological models have been proposed to capture the shear stress-shear rate relationships characteristic of non-Newtonian flows such as lahars. Among the most commonly used are the Manning formula and Manning-type expressions, which include dilatant and viscous adaptations (Vignaux and Weir 1990; Barberi et al. 1992; Costa 1997). The Voellmy friction model (Voellmy 1955) is also frequently employed, particularly for granular flow simulations (Pirulli and Sorbino 2008; Schraml et al. 2015), and has been used for lahar modelling as well (de' Michieli Vitturi et al. 2019; Franco-Ramos et al. 2020; Figueroa-García et al. 2021). This model expresses total flow resistance as the sum of turbulent friction and dry Coulombtype friction. Alternatively, the Bingham (1916) rheological model incorporates both yield and viscous stresses and is widely used for simulating the dynamic and static behaviour of mudflows (Dent and Lang 1983; Chen and Lee 2002; Pastor et al. 2014). This model defines a linear stress-strain relationship with a non-zero yield stress, where the intercept and slope correspond to the yield and viscous components, respectively. Other rheological formulations have also been applied to lahars, including those proposed by O'Brien and Julien (1988) and Herschel and Bulkley (1926).

Major challenges in lahar modelling using these approaches include high parameter uncertainty, scarce calibration data, and difficulties in accurately predicting flow paths in complex terrain topographies (e.g., Costa 1997, Haddad et al. 2010, Caballero and Capra 2014, Kheirkhah Gildeh et al. 2021). Particularly for the rheological models parameters, the values can range widely providing similar runout distance for different combination of the parameters.

This study aims to evaluate the performance of various rheological models in reconstructing the 2001 lahar event at Popocatépetl volcano (Mexico). Simulations were carried out using the non–Newtonian flow module of the hydrodynamic modelling tool Iber (Bladé *et al.* 2014a; Sanz-Ramos *et al.* 2025), which includes the most common rheological models used in lahar modelling.

# **STUDY SITE**

# Lahar-prone area: Huiloac gorge, Popocatépetl volcano

Popocatépetl volcano (Figure 1a), located in the Trans-Mexican Volcanic Belt (TMVB), is a stratovolcano approximately 70 km southeast of Mexico City and represents the second-highest peak in North America (~5400 m a.s.l.). Eruptive events can release and deposit large amounts of volcanic material, affecting both nearby slopes and distant lowland areas. In particular, tephra composed of fine particles such as lapilli and ash, depending on eruption magnitude and intensity, may promote lahar initiation when remobilized by water sources such as rainfall or snowmelt.

According to the National Institute of Statistics and Geography of Mexico (INEGI), one of the most lahar-prone regions on the northern flank of the Popocatépetl volcano is the Huiloac Gorge (Figure 1b), which poses a direct threat to nearby populated areas including Santiago Xalitzintla and San Nicolás de los Ranchos. The most recent significant lahar in this gorge occurred in 2001, likely initiated during an eruptive phase by a water input from partial melting of the summit glacier (Capra *et al.* 2004). This event exhibited distinctive flow characteristics influenced by its sand-to-silt particle size distribution and high water content, traveling approximately 12–13 km from the glacier source to the final depositional zone (Figure 1b, dashed line).

# Data available for the event

Accurate numerical reconstruction of lahar events requires two primary inputs: high-resolution topographic data to define the computational domain, and information on the material composition to appropriately characterize the rheological behaviour during the dynamic phase of the flow.

For this study, the most recent digital terrain model (DTM) available from the INEGI was employed. This raster-format DTM offers a horizontal resolution of 15 m and a mean global vertical Root Mean Square Error (RMSE) of 4.8 m.

The 2001 lahar was simulated by prescribing a discharge hydrograph as an inlet boundary condition at the uppermost point of the computational domain, located at approximately 3600 m a.s.l. The hydrograph was derived from the interpretation of geophone data recorded along the Huiloac Gorge (Capra *et al.* 2004; Muñoz-Salinas *et al.* 2007), and is characterized by a peak discharge of 335 m³/s and a duration of 3 h.

# NUMERICAL MODELLING TOOL

# Non-Newtonian module of Iber

Iber is a hydrodynamic numerical modelling tool initially developed for flood hazard and risk assessment (Bladé *et al.* 2014a, 2014b). Since its release in 2010, its application scope has broadened significantly to include morphodynamic processes, pollutant and sediment transport, large wood dynamics, hydrological and soil erosion modelling, urban drainage systems, and eco-hydraulics (*e.g.*,

Ruiz-Villanueva et al. 2014; Cea and Bladé 2015; Sanz-Ramos et al. 2019, 2022; Bladé et al. 2019; Aranda et al. 2021; Olivares-Cerpa et al. 2022; Innocenti et al. 2023; Costabile et al. 2024).

The tool has recently been enhanced with the incorporation of a new module, called Iber-NNF, which is specifically designed to simulate non-Newtonian shallow flows. This module was already used to simulate dense snow avalanches (Sanz-Ramos et al. 2021, 2023a), mudflows and mine tailings propagation after a dam-break (Sanz-Ramos et al. 2024a, 2024c) and wood-laden flows (Ruiz-Villanueva et al. 2019). In these non-Newtonian flows, the resistance forces, which are typically represented by the Manning or Chezy formulas in conventional hydraulics, are instead computed through a rheological model tailored to capture the unique properties of the flow. This approach allows for a more accurate representation of the dynamic behaviour of non-Newtonian fluids, where traditional hydraulic formulas are inadequate.

Iber-NNF, like Iber, solves the two-dimensional depth-averaged shallow water equations (2D-SWE) in a cartesian coordinate system (Equation (1)):

$$\begin{split} \frac{\partial h}{\partial t} + \frac{\partial q_x}{\partial x} + \frac{\partial q_y}{\partial y} &= 0\\ \frac{\partial q_x}{\partial t} + \frac{\partial}{\partial x} \left( \frac{q_x^2}{h} + g' k_p \frac{h^2}{2} \right) + \frac{\partial}{\partial y} \left( \frac{q_x q_y}{h} \right) &= g' h(S_{o,x} - S_{f,x})\\ \frac{\partial q_x}{\partial t} + \frac{\partial}{\partial x} \left( \frac{q_x q_y}{h} \right) + \frac{\partial}{\partial y} \left( \frac{q_y^2}{h} + g' k_p \frac{h^2}{2} \right) &= g' h(S_{o,y} - S_{f,y}) \end{split}$$
(1)

where h is the fluid depth,  $q_x$  and  $q_y$  are the two components of the specific discharge, g is the gravitational acceleration,  $S_{o,x}$  and  $S_{o,y}$  are the two bottom slope components, and  $S_{f,x}$  and  $S_{o,y}$  are the two friction slope components of the rheological model.

The 2D-SWE were adapted to simulate non-Newtonian shallow flows in a global coordinate system in steep slopes ( $g' = g \cos^2 \theta$ ), with a non-hydrostatic pressure distribution  $(k_p)$  and using a rheological model as frictional terms. To achieve this, a particular numerical scheme was implemented, ensuring the balance among the different terms of the 2D-SWE and the stop of the fluid according to the rheological properties of the fluid, even in steep slopes and complex geometries (Sanz-Ramos et al. 2023a).

# Rheological models

The current version of Iber implements eight rheological models: Manning, Viscous, Dilatant, Voellmy, Bartelt, Bingham (simplified), O'Brien-Julien (also called 'quadratic') and Herschel-Bulkley. All of these rheological models have been previously used in lahar simulations (e.g., Macedonio and Pareschi 1992; Costa 1997; Haddad et al. 2010; Franco-Ramos et al. 2020; Martínez-Valdés et al. 2023; Satria et al. 2024), except Bartelt. These models, expressed as friction slope ( $S_{\theta}$  which is related to the shear stress as  $\tau = \rho g h S_{\theta}$ ), are described below:

Manning (Chow 1959): 
$$S_f = \frac{n^2 v^2}{h^{4/3}}$$
 (2)

Viscous (Macedonio and Pareschi 1992): 
$$S_f = \frac{n^2 v^2}{h^3}$$
 (3)

Dilatant (Macedonio and Pareschi 1992): 
$$S_f = \frac{n^2 v}{h^2}$$
 (4)

Dilatant (Macedonio and Pareschi 1992): 
$$S_f = \frac{h^2}{h^2}$$
 (4)  
Bingham simplified:  $S_f = \frac{1}{\rho gh} \left( \omega \tau_y + 3 \frac{\mu_B \nu}{h} \right)$  (5)  
Voellmy (1955):  $S_f = \frac{\nu^2}{\xi h} + \mu$  (6)

Voellmy (1955): 
$$S_f = \frac{v}{\xi h} + \mu \tag{6}$$

Bartelt *et al.* (2015): 
$$S_{f} = \frac{1}{\rho gh} \left( C \left( 1 - \mu \right) \left( 1 - e^{\frac{1}{\rho gh}} \right) \right)$$
 (7)
O'Brien and Julien (1988): 
$$S_{f} = \frac{\tau_{y}}{\rho gh} + \frac{K \mu_{B} \nu}{8 \rho g h^{2}} + \frac{n^{2} \nu^{2}}{h^{4/3}}$$
 (8)

O'Brien and Julien (1988): 
$$S_{f} = \frac{t_{y}}{\rho g h} + \frac{R \mu_{B} v}{8 \rho g h^{2}} + \frac{n^{2} v^{2}}{h^{4/3}}$$
 (8)

Herschel and Bulkley (1926): 
$$S_{f} = \frac{1}{\rho gh} \left( \tau_{y} + k \left( \frac{\nu}{h} \right)^{\alpha} \right)$$
 (9)

where the calibration parameters of each rheological model are the flow density  $(\rho)$ , the Manning coefficient (n), the yield stress  $(\tau_v)$ , the fluid viscosity ( $\mu_B$ ), the Coulomb friction coefficient ( $\mu$ ), the turbulent friction coefficient ( $\xi$ ), the cohesion (C), a resistance parameter (K), a consistency parameter (k), and the shear power  $(\alpha)$ .

The Coulomb model, which is often used either independently or in combination with other rheological models in lahar simulations (Pitman et al. 2003; Tierz et al. 2017; Kmetyko et al. 2024), can be represented by the Voellmy model with  $\xi \rightarrow \infty$ , effectively eliminating the contribution of the viscous term. Furthermore, the yield slope term in the simplified Bingham model is modified by  $\omega$ , a factor that accommodates the different formulations found in the literature for this parameter (Chen and Lee 2002; Pitman et al. 2003; Sanz-Ramos et al. 2024a). The Bartelt rheological model was excluded from this study, as it was originally developed to account for cohesion forces in

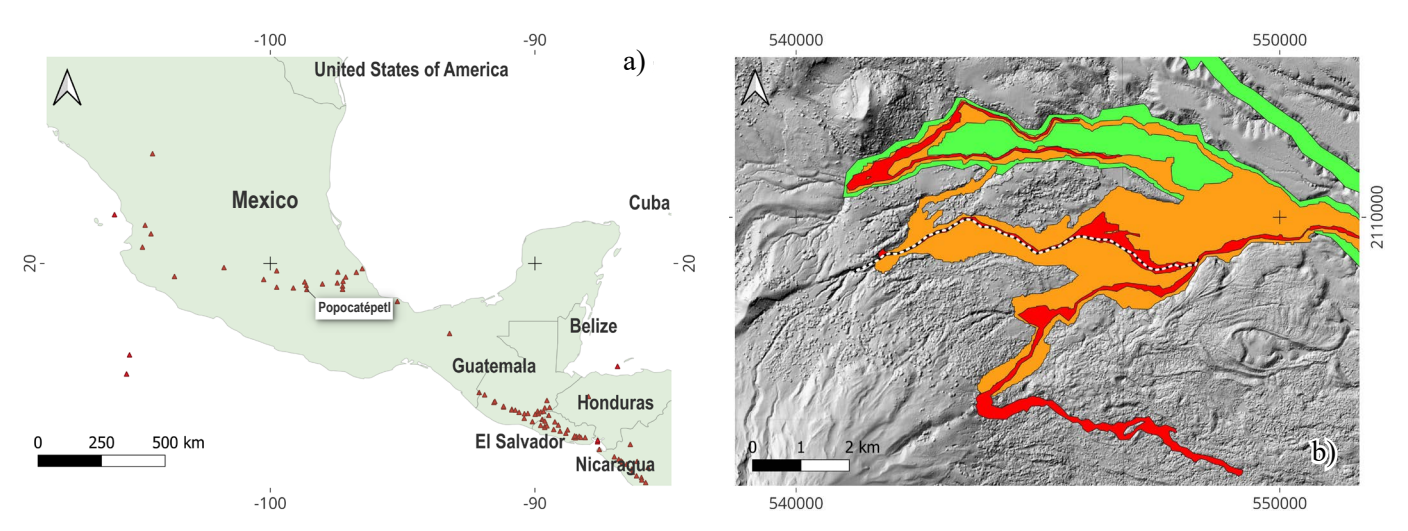


Figure 1. (a) Location of Popocatépetl volcano in the TMVB (EPSG: 4326). (b) Probability lahar maps (high: red; moderate: orange; low: green) according to Martin Del Pozzo et al. (2017) and lahar 2001 runout within Huiloac Gorge (dashed line) according to Capra et al. (2004) (EPSG: 32614).

snow avalanche modelling (Bartelt *et al.* 2015) in conjunction with the Voellmy model, although it may also be used independently.

# Model setup

The study area covered 1774 ha, with elevations ranging from 3600 to 2500 m a.s.l. The domain was discretized using a mesh of 180000 triangular elements, each with an average side length of 15 m, corresponding to the resolution of the digital terrain model (DTM). The maximum simulation time was set to five hours.

Following the methodology outlined by Caballero and Capra (2014), the hydrograph was applied at the highest elevation, with a fluid density of 1740 kg/m<sup>3</sup>. A pressure factor ( $k_p$ ) of 1 was used, as the lahar had already been triggered and fluidized, and thus the hydrograph was employed rather than an initial condition.

The rheological model parameters were adjusted (Table 1) to replicate the maximum runout distance of the 2001 Popocatépetl lahar, as estimated by Capra *et al.* (2004). Parameters affecting the velocity-dependent terms of the rheological model were assumed to be homogeneous across the domain, although Iber allows for spatial distribution through manual or raster assignment. Other parameters, primarily related to the physical properties of the fluid, were treated as constant values throughout the simulation.

# **RESULTS**

# General behaviour and flood extent

Figure 2 illustrates, through the map of maximum flow depths, the maximum extent of the lahar according to the parameters of the five rheological models tested. It is worth noticing that the Manning model was used as a representative formula for the Viscous and Dilatant models, as their expressions are derived from Manning-like formulas, which are expected to produce similar hydrodynamic behaviour.

Rheological models that implement only velocity-dependent terms, such as the Manning-like models, were unable to halt the fluid flow, either on flat or steep slopes. This is evident in Figure 2a, where the flood extent is larger—similar to hydraulic modelling results—and the fluid continues to flow downstream and leaving the model domain. Several branches emerged due to high inertial terms, causing the fluid to overtop the gorge banks, which partially flooded adjacent gorges and streams. Maximum flow depths up to 5 m were obtained at the upstream sections and the maximum flood extent was greater than 718 ha.

The remaining rheological models displayed similar behaviour in terms of flooded area, with runouts consistent with observations (Figure 2, red-orange triangle). The Voellmy model (Figure 2b) exhibited the second-largest flood extension (149 ha), along with a significant deposition area with more than 5 m depth on the left floodplain, which formed when the gorge width expanded in the mid-lower stream. This flooded area is similar to those identified as 'high hazard zone' (Martin Del Pozzo *et al.* 2017), predominantly extending to the north (Figure 2, yellow polygon).

The results from the Bingham, O'Brien-Julien, and Herschel-Bulkley models were generally comparable. The flood extent of the Bingham model was smaller than the others (65 ha), yet all three models indicated similar maximum depths along the gorge ( $\sim$ 4 m), with a tendency to flood the area just before the gorge widens in the mid-stream section. As with the Voellmy model, the flow predominantly affected the northern portion of the mid-lower stream. Results from O'Brien-Julien and Herschel-Bulkley were almost identical, with a flood extent of 74 ha and 88 ha and maximum flow depths of 4.0 and 4.8 m, respectively.

# Time arrival and flow velocity

The simulated arrival time to the farthest deposition point of the 2001 Popocatépetl lahar by the different rheological models varied slightly. The Manning model arrived in less than 0:30 hours, even using a Manning coefficient of 1 s/m<sup>1/3</sup>. Voellmy and Bingham models exhibited the slowest front velocity, with an arrival time between 3:40 and 3:50 hours. In contrast, the Herschel-Bulkley model displayed the fastest propagation, with an arrival time of 2:50–3:00 hours. The O'Brien-Julien model showed intermediate arrival times, ranging from 3:00 to 3:10 hours. Notably, once the lahar reached the farthest deposition point, it ceased movement across all rheological models, maintaining a non-horizontal free surface. This behaviour was not obtained with the Manning rheological model, as the lahar continued flowing downstream reaching the limits of the model.

Results of the simulated velocity were compared to the lahar velocity estimated by Muñoz-Salinas *et al.* (2007) using the superelevation technique at the mid-lower part of the runout area. Generally, Iber-NNF correctly captured the estimated velocity at the nine points evaluated (Table 2). The Manning model generally underestimated the maximum velocity at the control points since the flow was spilled over a larger area, i.e., the flow did not concentrate in the gorge. Voellmy model presented larger velocities in all sections, in accordance with the fastest arrival time, while the maximum runout distance was well captured. This behaviour was caused by the lower contribution of the Coulomb term in resistance forces. Bingham model provided moderate flow velocities, similar to those presented by Muñoz-Salinas. Finally, O'Brien-Julien and Herschel-Bulkley presented the slowest flow velocities in all sections, in agreement with the arrival time.

# **DISCUSSION**

# Rheological models and parameters range

The parameters of the rheological model are the primary factors governing energy dissipation resulting from flow-boundary interactions, as flow turbulence is typically not considered in lahar simulations using SWE-based numerical tools. Therefore, selecting appropriate values for these parameters is crucial for obtaining reliable results.

Table 3 presents a comparison between the parameters used in the simulations and the minimum and maximum values found in the literature for lahar and debris flow modelling. In general, the values of the parameters of the rheological models tested in the numerical reconstruction of the 2001 Popocatépetl lahar are within the typical range used in lahar simulations. However, some values of the O'Brien-

Table 1. Values of the parameters of the rheological models used to simulate the Popocatépetl lahar.

| Manning                    | Voellmy     |          | Bingham |                  | O'Brien-Julien |                |          |                            | Herschel-Bulkley       |                           |          |
|----------------------------|-------------|----------|---------|------------------|----------------|----------------|----------|----------------------------|------------------------|---------------------------|----------|
| n<br>(s/m <sup>1/3</sup> ) | ξ<br>(m/s²) | μ<br>(-) |         | $\mu_{B}$ (Pa·s) |                | $\mu_B$ (Pa·s) | K<br>(-) | n<br>(s/m <sup>1/3</sup> ) | τ <sub>y</sub><br>(Pa) | k<br>(Pa⋅s <sup>α</sup> ) | α<br>(-) |
| 1                          | 2000        | 0.05     | 600     | 500              | 700            | 5              | 2000     | 0.06                       | 600                    | 1500                      | 0.5      |

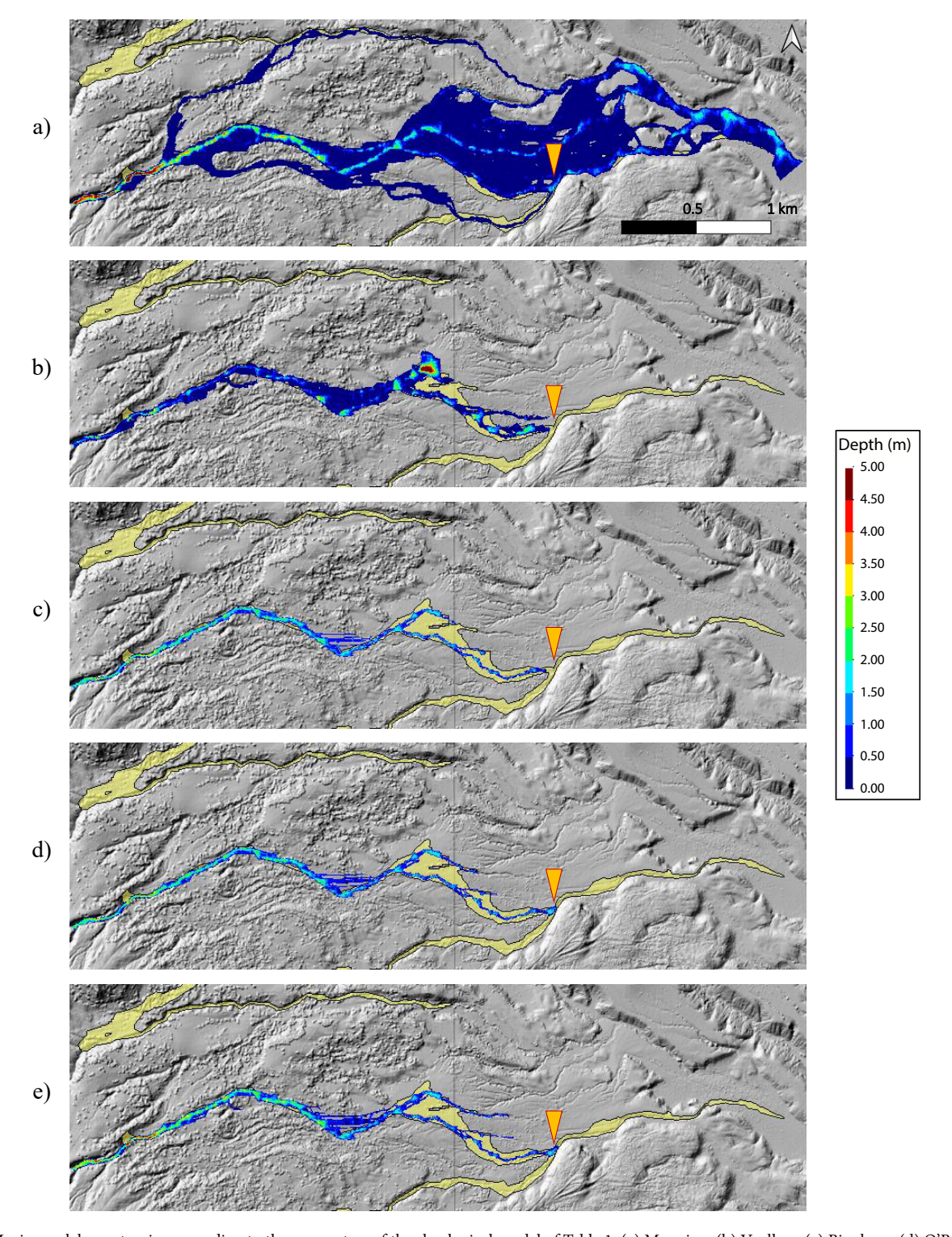


Figure 2. Maximum lahar extension according to the parameters of the rheological model of Table 1: (a) Manning, (b) Voellmy, (c) Bingham, (d) O'Brien-Julien, and (e) Herschel-Bulkley. High lahar hazard zone according to Martin Del Pozzo *et al.* (2017): yellow polygon. Symbol verpresents the farthest deposition point of the 2001 Popocatépetl lahar (548315,2109126; EPSG: 32614).

Julien and Herschel-Bulkley models, particularly those related to the non-velocity-dependent term and the factor multiplying the velocity term, deviate from those commonly used. The values proposed for these models resulted in lower resistance, causing the flow to exit the model domain, similar to the behaviour observed with Manning-like models.

For the Manning and Voellmy models, numerous handbooks and guidelines provide recommended values, particularly in hydraulic engineering (Arcement and Schneider 1989) and in snow avalanches modelling (Buser and Frutiger 1980; Bakkehøi *et al.* 1981; Brugnot 2000), where the flow behaves similarly to non-Newtonian shallow flow. Although Manning-like models were unable to halt fluid

movement over irregular and steep slopes, they continue to be used in lahar modelling (*e.g.*, Syarifuddin *et al.* 2018; Vera *et al.* 2019; Bonasia *et al.* 2022) using values of *n* out of the common range for hydraulics. The values used in the current research emphasise the fact that the resistance forces computed through rheological models are parameters to calibrate, as well as the Manning coefficient in hydraulics.

Recently, the Voellmy model has emerged as an alternative to other rheological models for lahar simulations (e.g., Franco-Ramos et al. 2020; Figueroa-García et al. 2021). The Coulomb friction coefficient  $(\mu)$  demonstrated to be highly sensitive to variations in this case study due to topographic irregularities within the gorge, such as sinks and barriers (Muñoz-Salinas et al. 2008), which tend to accumulate the flow for mid-high values of  $\mu$  (a parameter directly related to the basal friction angle). Values greater than 0.15 notably increase the basal friction and, thus, the total resistance forces. In such cases, the fluid tends to accumulate in the upstream area without reaching the deposition area. However, lower values are physically possible since this parameter is directly related to the angle of repose, which it can be less than 0.15 for sediment-laden flows with high concentrations of water (e.g., mudflows). When using the 'fill sinks' option in GIS software or Iber (see next section), the topography is notably modified, and consequently, the rheological parameters should also be adjusted to align with the observed results, particularly increasing  $\mu$  in such cases. On the other hand, the turbulent friction coefficient ( $\xi$ ) used is within the typical values found in the literature. It is not a physically based parameter, but it can be related to the Chezy coefficient (Ruiz-Villanueva et al. 2019; Sanz-Ramos et al. 2023b).

The Bingham model has proven useful for simulating mudflows under low shear rates, where both yield and viscous stresses depend on the cohesion of fine sediments, as well as for simulating debris flows (Dent and Lang 1982; O'Brien *et al.* 1993; Cordonnier *et al.* 2016; Msheik 2020; Thouret *et al.* 2020; Kheirkhah Gildeh *et al.* 2021). However, there are few applications of this model for lahar simulations as the sole rheological model (Haddad *et al.* 2010, 2016). Table 3 also shows the typical values used in debris flow modelling, highlighting that the value of the yield stress  $(\tau_y)$  used is close to the minimum value commonly used for debris flows.

The O'Brien-Julien model incorporates elements from previous rheological models into a quadratic equation for velocity-dependent terms. It has been widely applied in lahar modelling due to the availability of a parameter database for its selection (O'Brien and Julien 1988). Nevertheless, these parameters were derived initially for mudflows with specific particle sizes and characteristics (*e.g.*, silts and clays) in laboratory settings. As such, they may not be optimal for representing the properties of lahar materials and could require adjustment to achieve the best fit with field observations. The values of the yield stress ( $\tau_y$ ) and the fluid viscosity ( $\mu_B$ ) used in this study are out of the standard range used for lahar modelling, but within the

range for debris flow modelling. The performance of this rheological model in Iber-NNF was proven to be adequate for mine-tailing flow propagation (Sanz-Ramos *et al.* 2024a). So, assuming a flow depth and velocity of 1 m and 1 m/s, we can demonstrate that the contribution of these two parameters to the friction slope is very low  $(S_f(\tau_y, \mu_B) < 0.005$ , while  $S_f(n) > 0.15$ ), even for the maximum values commonly used.

# The influence of topography resolution on the simulation extent

The reconstruction of the 2001 Popocatépetl lahar was carried out using a Digital Terrain Model (DTM) with a 15 m cell size. However, other XY resolutions were also available and tested, including 5, 30, 60, 90, and 120 m cell size. The event was re-simulated, maintaining the mesh resolution and rheological parameters from Table 1, but using different topographical data. For sake of simplicity, the description of this analysis will focus here on the Bingham model, although similar behaviour was obtained with the other rheological models.

Figure 3 shows the maximum extent of the lahar using DTMs with varying resolutions. Coarser DTMs, such as those with 120 m (Figure 3a) and 90 m (Figure 3b) cell size, provided the poorest results. In these cases, the gorge geometry appeared smoother, leading to less accurate representation of the flow path. The fluid tended to continue flowing in a straight line, as the gorge was not sufficiently defined. From DTMs of 60 (Figure 3c) to 30 m (Figure 3d) cell size, the lahar flow developed branches, more closely matching the 'high hazard zone' (yellow polygon). However, the runout was slightly shorter than observed (~600–800 m).

The use of 5 m cell size DTM provided mixed results. The original DTM (Figure 3e), without using the 'fill sinks' option of Iber (Sanz-Ramos *et al.* 2020), resulted in a much smaller runout distance than using the enhanced DTM with the 'fill sinks' option (Figure 3f), which exceeded in ~1000 m the detention point observed by Capra *et al.* (2004). Despite the 5 m cell size DTM should provide a more detailed channel information, the use of a coarser mesh (15 m side size) generated numerical sinks and barriers that prevented the flow form flowing downstream.

Figure 3 also presents the estimated extent of 'high hazard zone' in Popocatépetl (yellow polygons) presented by Martin Del Pozzo *et al.* (2017). While the topographical data and methodology used to generate these hazard maps differ from those applied in this study, the results of the numerical model are consistent with the rheological model and the observed dynamics of the lahar flow. Overall, the simulated flood-prone areas align with the extent of the hazard maps for low-probability lahars. It is important to note that the hazard map for the Huiloac Gorge overlaps with another stream originating from the south. Therefore, lahar modelling should account for the potential triggering of concurrent lahars from different regions that converge at this location.

Table 2. Comparison between the flow velocity estimated by Muñoz-Salinas  $et\ al.$  (2007) and the simulated velocity according to each rheological model tested.

| X      | Y       | Muñoz-Salinas  | Manning | Voellmy | Bingham                       | O'Brien-Julien | Herschel-Bulkley |
|--------|---------|----------------|---------|---------|-------------------------------|----------------|------------------|
|        |         | $ \mathbf{v} $ |         |         | $ \mathbf{v} _{\mathrm{sim}}$ |                |                  |
|        |         | (m/s)          |         |         | (m/s)                         |                |                  |
| 541045 | 2108914 | 4.9            | 1.5     | 8.3     | 4.3                           | 3.6            | 2.1              |
| 541635 | 2109173 | 13.8           | 13.5    | 13.5    | 14.8                          | 8.1            | 11.8             |
| 542002 | 2109317 | 4.7            | 0.9     | 9.2     | 4.7                           | 4.0            | 2.1              |
| 542821 | 2109711 | 6.3            | 2.7     | 10.0    | 4.5                           | 3.4            | 2.1              |
| 543408 | 2109474 | 1.6            | 1.1     | 8.5     | 1.4                           | 1.6            | 1.3              |
| 543543 | 2109724 | 1.5            | 2.5     | 3.9     | 1.3                           | 1.5            | 1.4              |

Table 3. Values of the parameters of the rheological model used in Iber-NNF and range for lahar modelling.

| Model            | Variable                                   | Value | Range fo | or lahars | Range for debris |      |  |
|------------------|--|-------|----------|-----------|------------------|------|--|
|                  | (units)                                    |       | Min.     | Max.      | Min.             | Max. |  |
| Manning          | n (s/m <sup>1/3</sup> )                    | 1     | 0.15     | 1.09      | 0.1              | 1    |  |
| Voellmy          | $\xi$ (m/s <sup>2</sup> )                  | 1500  | 300      | 5000      | 10               | 600  |  |
|                  | μ (-)                                      | 0.05  | 0.15     | 0.50      | 0.1              | 0.55 |  |
| Bingham          | $\tau_{y}$ (Pa)                            | 600   | 60       | 600       | 750              | 3500 |  |
|                  | $\mu_B$ (Pa·s)                             | 500   | 50       | 500       | 0.4              | 3200 |  |
| O'Brien-Julien   | $\tau_y$ (Pa)                              | 700   | 0.192    | 35.7      | 700              | 1500 |  |
|                  | $\mu_B$ (Pa·s)                             | 5     | 0.0137   | 0.144     | 5                | 35   |  |
|                  | K (-)                                      | 2000  | 400      | 2000      | 24               | 2000 |  |
|                  | $n (s/m^{1/3})$                            | 0.06  | 0.065    | 0.167     | 0.05             | 0.20 |  |
|                  | $C_{v}\left( -\right)$                     | 0.45  | 0.20     | 0.66      | 0.3              | 0.6  |  |
|                  | $F_{r, max}(-)$                            | 0.9   | 0.9      | 0.9       | 0.5              | 2    |  |
| Herschel-Bulkley | $\tau_y$ (Pa)                              | 600   | 0.0239*  | 0.0239*   |                  |      |  |
|                  | $k$ (Pa·s <sup><math>\alpha</math></sup> ) | 1500  | 2.76*    | 2.76*     |                  |      |  |
|                  | α (-)                                      | 0.5   | 0.5*     | 0.5*      |                  |      |  |

\*Data provided without units in Satria et al. (2024).

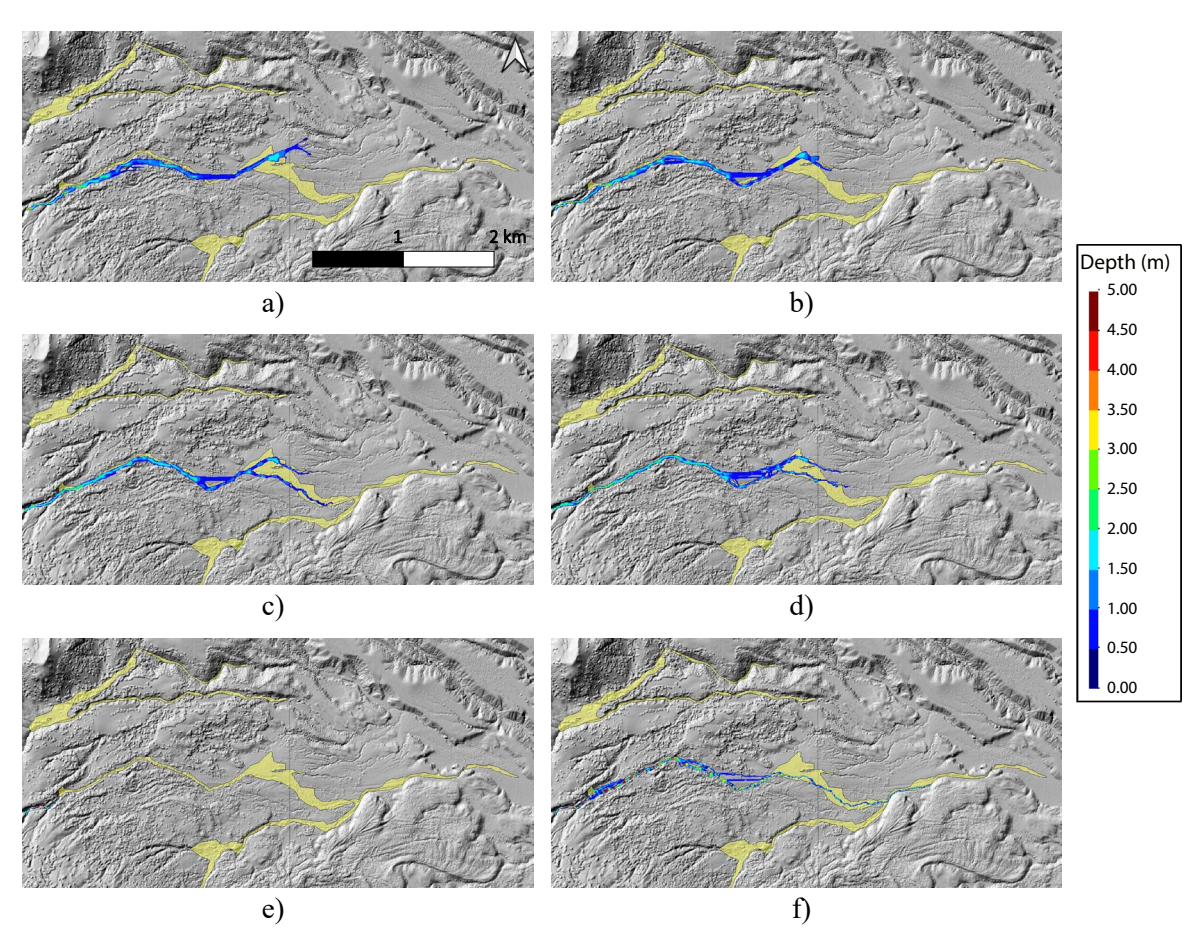


Figure 3. Variations on the maximum lahar extension according the DTM used: (a) 120 m cell size, (b) 90 m cell size, (c) 60 m cell size, (d) 30 m cell size, (e) 5 m cell size without 'fill sinks', and (f) 5 m cell size with 'fill sinks'. High lahar hazard according to Martin Del Pozzo *et al.* (2017): yellow polygon.

# Performance of the numerical tool

The results of the 2001 lahar simulation using Iber are consistent with the selected rheological model parameters and the employed topographical data. With the exception of the Manning model—which incorporates only a velocity-dependent resistance term—all simulations resulted in flow cessation and deposition over irregular

terrain with a non-horizontal free surface. The model successfully reproduced the observed runout of the 2001 lahar using several rheological models, underscoring the importance of model selection and the fact that different parameter sets—and even different rheological models—can yield comparable outcomes (Sanz-Ramos *et al.* 2023b).

The computational time of each simulation was completed in less than 10 minutes, attributable to the relatively coarse mesh (mean side length of 15 m), which allowed for larger time steps while satisfying the Courant–Friedrichs–Lewy condition (Courant *et al.* 1967). Notably, simulations using the Manning model required greater computational time due to high velocities and increased wetted elements, which elevate computational demands. Although runtimes were modest for the 2001 Popocatépetl lahar case, adopting finer topographic data and mesh resolution would significantly increase computation time. To address this, future versions of Iber-NNF are planned to support GPU-based parallel computing—similar to the sediment transport and habitat modules—offering speed-ups of over 100 times (Sanz-Ramos *et al.* 2023c, 2024b; Dehghan-Souraki *et al.* 2024; López-Gómez *et al.* 2024).

# **CONCLUSIONS**

Numerical modelling of lahars presents significant challenges due to their complex flow behaviour and the inherent difficulties associated with field data acquisition. Nevertheless, accurate modelling is essential for lahar hazard and risk assessment, as well as to develop of effective mitigation strategies. In this study, the hydrodynamic modelling tool Iber—specifically its non-Newtonian module, Iber-NNF—was employed to simulate the 2001 lahar event at Popocatépetl volcano using different rheological models. The results highlight the critical role of rheological model selection in accurately capturing both the dynamic and depositional (static) phases of lahar flow. Among the models tested, Manning-like formulations (Manning, Viscous, and Dilatant) exhibited the weakest performance, as they rely solely on velocity-dependent resistance terms that act only during flow motion, failing to adequately represent flow cessation and deposition.

**Acknowledgements.** The revised version benefits from the comments of two anonymous reviewers.

Author contributions. M.S.R. Methodology, research, data processing, analysis and interpretation, writing, revision, editing, resources; E.B. Methodology, research, revision, resources; A.D.H. Methodology, research, data processing, analysis and interpretation, writing, revision, resources; D.V.T. Data analysis and interpretation, revision, resources; J.G. Writing, revision, editing; N.S. Revision, editing, resources; I.G. Revision, editing, resources. All authors discussed the results and contributed to the manuscript.

**Data avaliability statement.** The authors declare that all data/part of the topography data, lahar hazard map and data from the 2001 Popocatépetl lahar event that support the findings of this study are available with open access from INEGI (https://www.inegi.org. mx/), Del Pozzo *et al.*, 2017 (https://www.geofisica.unam.mx/assets/monografias22.pdf) and Capra *et al.*, 2004 (https://doi.org/10.1016/S0377-0273(03)00413-X), as well as the Iber simulation tool (www.iberaula.com).

Declaration of Competing Interests. The authors declare that they are not aware of any financial conflicts of interest or personal relationships that could have influenced the work reported in this article. Funding. This publication is part of the Proyecto Especial Intramural (PIE) «Investigación geológica de la erupción de 2021 en Cumbre Vieja» (reference 20223PAL002), funded by the Consejo Superior de Investigaciones Científicas (CSIC),, and the project «Investigación geológica dirigida a la recuperación de la isla de La Palma tras la erupción volcánica de 2021» (GEOPALMA), funded by the Consejería de Transición Ecológica, Lucha contra el Cambio Climático y Energía del Gobierno de Canarias (reference 227G0165) and the Secretaría de Estado de Medio Ambiente.

# **REFERENCES**

- Aranda, J. Á, Beneyto, C., Sánchez-Juny, M., Bladé, E. (2021). Efficient Design of Road Drainage Systems. *Water*, 13(12), 1661. https://doi.org/10.3390/w13121661
- Arcement, G. J., & Schneider, V. R. (1989). Guide for selecting Manning's roughness coefficients for natural channels and flood plains. *United States Geological Survey Water-Supply Paper 2339*. https://doi. org/10.3133/wsp2339
- Bakkehøi, S., Cheng, T., Domaas, U., Lied, K., Perla, R., & Schieldrop, B. (1981). On the computation of parameters that model snow avalanche motion. *Canadian Geotechnical Journal*, 18(1), 121–130. https://doi. org/10.1139/t81-011
- Barberi, F., Caruso, P., Macedonio, G., Pareschi, M. T., & Rosi, M. (1992). Reconstruction and numerical simulation of the lahar of the 1877 eruption of Cotopaxi volcano (Ecuador). Acta Vulcanologica, 2, 35–44.
- Bartelt, P., Valero, C. V., Feistl, T., Christen, M., Bühler, Y., & Buser, O. (2015). Modelling cohesion in snow avalanche flow. *Journal of Glaciology*, 61(229), 837–850. https://doi.org/10.3189/2015JoG14J126
- Bingham, E. C. (1916). An investigation of the laws of plastic flow. *Bulletin of the Bureau of Standards*, 13(2), 309–353. https://doi.org/10.6028/bulletin.304
- Bladé, E., Cea, L., Corestein, G., Escolano, E., Puertas, J., Vázquez-Cendón, E., Dolz, J., & Coll, A. (2014a). Iber: herramienta de simulación numérica del flujo en ríos. Revista Internacional de Métodos Numéricos Para Cálculo y Diseño En Ingeniería, 30(1), 1–10. https://doi.org/10.1016/j. rimni.2012.07.004
- Bladé, E., Cea, L., & Corestein, G. (2014b). Modelización numérica de inundaciones fluviales. *Ingeniería Del Agua*, 18(1), 68. https://doi. org/10.4995/ia.2014.3144
- Bladé, E., Sánchez-Juny, M., Arbat, M., & Dolz, J. (2019). Computational Modeling of Fine Sediment Relocation Within a Dam Reservoir by Means of Artificial Flood Generation in a Reservoir Cascade. Water Resources Research, 55(4), 3156–3170. https://doi.org/10.1029/2018WR024434
- Bonasia, R., Turchi, A., Madonia, P., Fornaciai, A., Favalli, M., Gioia, A., & Traglia, F. Di. (2022). Modelling Erosion and Floods in Volcanic Environment: The Case Study of the Island of Vulcano (Aeolian Archipelago, Italy). Sustainability, 14(24), 16549. https://doi.org/10.3390/ su142416549
- Brugnot, G. (2000). SAME Avalanche mapping, model validation and warning systems. Office for European Commission. Official Publications of the European Communities, Luxemburg.
- Buser, O., & Frutiger, H. (1980). Observed Maximum Run-Out Distance of Snow Avalanches and the Determination of the Friction Coefficients  $\mu$  and  $\xi$ . *Journal of Glaciology*, 26(94), 121–130. https://doi.org/10.3189/S0022143000010662
- Caballero, L., & Capra, L. (2014). The use of FLO2D numerical code in lahar hazard evaluation at Popocatépetl volcano: a 2001 lahar scenario. Natural Hazards and Earth System Sciences, 14(12), 3345–3355. https://doi.org/10.5194/nhess-14-3345-2014
- Capra, L., Poblete, M. A., & Alvarado, R. (2004). The 1997 and 2001 lahars of Popocatépetl volcano (Central Mexico): textural and sedimentological constraints on their origin and hazards. *Journal of Volcanology and Geothermal Research*, 131(3-4), 351-369. https://doi.org/10.1016/ S0377-0273(03)00413-X
- Cea, L., & Bladé, E. (2015). A simple and efficient unstructured finite volume scheme for solving the shallow water equations in overland flow applications. Water Resources Research, 51(7), 5464–5486. https://doi. org/10.1002/2014WR016547
- Chen, H., & Lee, C. F. (2002). Runout Analysis of Slurry Flows with Bingham Model. *Journal of Geotechnical and Geoenvironmental Engineering*, 128(12), 1032–1042. https://doi.org/10.1061/(ASCE)1090-0241(2002)128:12(1032)
- Chow, V. Te. (1959). Open-Channel Hydraulics. In Open Channel Hydraulics. McGraw-Hill Book Company Inc. New York, USA.
- Cordonnier, B., Lev, E., & Garel, F. (2016). Benchmarking lava-flow models. Geological Society Special Publication, 426(1), 425–445. https://doi. org/10.1144/SP426.7
- Costa, J. E. (1997). Hydraulic modeling for lahar hazards at cascades

- volcanoes. Environmental and Engineering Geoscience, 3(1), 21–30. https://doi.org/10.2113/gseegeosci.iii.1.21
- Costabile, P., Cea, L., Barbaro, G., Costanzo, C., Llena, M., & Vericat, D. (2024). Evaluation of 2D hydrodynamic-based rainfall/runoff modelling for soil erosion assessment at a seasonal scale. *Journal of Hydrology*, 130778. https://doi.org/10.1016/j.jhydrol.2024.130778
- Courant, R., Friedrichs, K., & Lewy, H. (1967). On the partial difference equations of mathematical physics. IBM Journal of Research and Development, 11, 215–234.
- Darnell, A. R., Phillips, J. C., Barclay, J., Herd, R. A., Lovett, A. A., & Cole, P. D. (2013). Developing a simplified geographical information system approach to dilute lahar modelling for rapid hazard assessment. *Bulletin of Volcanology*, 75(4), 713. https://doi.org/10.1007/s00445-013-0713-6
- de' Michieli Vitturi, M., Esposti Ongaro, T., Lari, G., & Aravena, A. (2019). IMEX\_SfloW2D 1.0: a depth-averaged numerical flow model for pyroclastic avalanches. Geoscientific Model Development, 12(1), 581– 595. https://doi.org/10.5194/gmd-12-581-2019
- Dehghan-Souraki, D., López-Gómez, D., Bladé-Castellet, E., Larese, A., & Sanz-Ramos, M. (2024). Optimizing sediment transport models by using the Monte Carlo simulation and deep neural network (DNN):

  A case study of the Riba-Roja reservoir. *Environmental Modelling & Software*, 175, 105979. https://doi.org/10.1016/j.envsoft.2024.105979
- Dent, J. D., & Lang, T. E. (1982). Experiments on mechanics of flowing snow. Cold Regions Science and Technology, 5(3), 253–258. https://doi. org/10.1016/0165-232X(82)90018-0
- Dent, J. D., & Lang, T. E. (1983). A Biviscous Modified Bingham Model of Snow Avalanche Motion. Annals of Glaciology, 4, 42–46. https://doi. org/10.3189/S0260305500005218
- Figueroa-García, J. E., Franco-Ramos, O., Bodoque, J. M., Ballesteros-Cánovas, J. A., & Vázquez-Selem, L. (2021). Long-term lahar reconstruction in Jamapa Gorge, Pico de Orizaba (Mexico) based on botanical evidence and numerical modelling. *Landslides*, 18(10), 3381– 3392. https://doi.org/10.1007/s10346-021-01716-3
- Franco-Ramos, O., Ballesteros-Cánovas, J. A., Figueroa-García, J. E., Vázquez-Selem, L., Stoffel, M., & Caballero, L. (2020). Modelling the 2012 Lahar in a Sector of Jamapa Gorge (Pico de Orizaba Volcano, Mexico) Using RAMMS and Tree-Ring Evidence. *Water*, 12(2), 333. https://doi.org/10.3390/w12020333
- Guerrero, A., Criollo, R., Córdoba, G., & Rodríguez, D. (2019). A Modeling Approach for Lahar Hazard Assessment: the Case of Tamasagra Sector in the City of Pasto, Colombia. *Ingeniería y Ciencia*, 15(30), 7–31. https://doi.org/10.17230/ingciencia.15.30.1
- Haddad, B., Pastor, M., Palacios, D., & Muñoz-Salinas, E. (2010). A SPH depth integrated model for Popocatépetl 2001 lahar (Mexico): Sensitivity analysis and runout simulation. *Engineering Geology*, 114(3-4), 312– 329. https://doi.org/10.1016/j.enggeo.2010.05.009
- Haddad, B., Palacios, D., Pastor, M., & Zamorano, J. J. (2016). Smoothed particle hydrodynamic modeling of volcanic debris flows: Application to Huiloac Gorge lahars (Popocatépetl volcano, Mexico). *Journal* of Volcanology and Geothermal Research, 324, 73–87. https://doi. org/10.1016/j.jvolgeores.2016.05.016
- Herschel, W. H., & Bulkley, R. (1926). Konsistenzmessungen von Gummi-Benzollösungen. *Kolloid-Zeitschrift*, 39(4), 291–300. https://doi.org/10.1007/bf01432034
- Huggel, C., Kääb, A., Haeberli, W., & Krummenacher, B. (2003). Regional-scale GIS-models for assessment of hazards from glacier lake outbursts: evaluation and application in the Swiss Alps. Natural Hazards and Earth System Sciences, 3(6), 647–662. https://doi.org/10.5194/nhess-3-647-2003
- Innocenti, L., Bladé, E., Sanz-Ramos, M., Ruiz-Villanueva, V., Solari, L., & Aberle, J. (2023). Two-Dimensional Numerical Modeling of Large Wood Transport in Bended Channels Considering Secondary Current Effects. Water Resources Research, 59(12). https://doi.org/10.1029/2022WR034363
- Kheirkhah Gildeh, H., Halliday, A., Arenas, A., & Zhang, H. (2021).
  Tailings Dam Breach Analysis: A Review of Methods, Practices, and Uncertainties. Mine Water and the Environment, 40(1), 128–150.
  https://doi.org/10.1007/s10230-020-00718-2
- Kmetyko, S., Mergili, M., & Palma, J. L. (2024). Numerical modelling of the lahars generated during the 2015 eruption at Volcán Villarrica

- (Chile). EGU General Assembly 2024, Vienna, Austria, 14–19 Apr 2024, EGU24-9844, 9844. https://doi.org/https://doi.org/10.5194/egusphere-egu24-9844
- López-Gómez, D., De Blas-Moncalvillo, M., Castejón-Zapata, M., Gassó-Sánchez, Á., Bladé, E., Sanz-Ramos, M., Dehghan-Souraki, D., Garrote-de Marco, L., Santillán-Sánchez, D., Soria-García, J. M., San Román-Saldaña, J., Galván-Plaza, R., García-Vera, M. Á., & Sánchez-Martínez, J. (2024). Análisis del transporte de sedimentos en el curso bajo del río Ebro mediante modelización numérica de una avenida controlada. *Ingeniería Del Agua*, 28(4), 246–262. https://doi.org/10.4995/ia.2024.21768
- Macedonio, G., & Pareschi, M. T. T. (1992). Numerical simulation of some lahars from Mount St. Helens. *Journal of Volcanology and Geothermal Research*, 54(1-2), 65-80. https://doi.org/10.1016/0377-0273(92)90115-T
- Martin Del Pozzo, A. L., Alatorre Ibargüengoitia, M., Arana Salinas, L., Bonasia, R., Capra Pedol, L., Cassata, W., Códoba, G., Cortés Ramos, J., Delgado Granados, H., Ferrés López, M., Fonseca Álvarez, R., García Reynoso, J. A., Gispert, G., Guerrero López, D. A., Jaimes Viera, M. C., Macías Vázquez, J. L., Nieto Obregón, J., Nieto Torres, A., Paredes Ruiz, P. A., ... Tellez Ugalde, E. (2017). Estudios geológicos y actualización del mapa de peligros del volcán Popocatépetl. Memoria técnica del mapa de peligros del volcán Popocatépetl. Monografías del Instituto de Geofísica. Universidad Nacional Autónoma de México. Instituto de Geofísica. México D.F., México.
- Martínez-Valdés, J. I., Márquez-Ramírez, V. H., Coviello, V., & Capra, L. (2023). Hurricane-induced lahars at Volcán de Colima (México): seismic characterization and numerical modeling. Revista Mexicana de Ciencias Geológicas, 40(1), 59–70. https://doi.org/10.22201/cgeo.20072902e.2023.1.1709
- Mead, S. R., & Magill, C. R. (2017). Probabilistic hazard modelling of rain-triggered lahars. *Journal of Applied Volcanology*, 6(1), 4–10. https://doi.org/10.1186/s13617-017-0060-y
- Msheik, K. (2020). Non-Newtonian Fluids: Modeling and Well-Posedness. Universite Grenoble Alpes, Saint-Martin-d'Hères, France.
- Muñoz-Salinas, E., Manea, V. C., Palacios, D., & Castillo-Rodriguez, M. (2007). Estimation of lahar flow velocity on Popocatépetl volcano (Mexico). *Geomorphology*, 92(1-2), 91-99. https://doi.org/10.1016/j.geomorph.2007.02.011
- Muñoz-Salinas, E., Renschler, C. S., Palacios, D., & Namikawa, L. M. (2008).
  Updating channel morphology in digital elevation models: Lahar assessment for Tenenepanco-Huiloac Gorge, Popocatépetl volcano, Mexico. Natural Hazards, 45(2), 309–320. https://doi.org/10.1007/s11069-007-9162-x
- O'Brien, J. S., & Julien, P. Y. (1988). Laboratory Analysis of Mudflow Properties. *Journal of Hydraulic Engineering*, 114(8), 877–887. https://doi.org/10.1061/(ASCE)0733-9429(1988)114:8(877)
- O'Brien, J. S., Julien, P. Y., & Fullerton, W. T. (1993). Two Dimensional Water Flood and Mudflow Simulation. *Journal of Hydraulic Engineering*, 119(2), 244–261. https://doi.org/10.1061/(ASCE)0733-9429(1993)119:2(244)
- Olivares-Cerpa, G., Russo, B., Martínez-Puentes, M., Bladé, E., & Sanz-Ramos, M. (2022). "SUDS-lineales" para reducir el riesgo de inundación considerando escenarios de Cambio Climático. *Ingeniería Del Agua*, 26(2), 77–90. https://doi.org/10.4995/ia.2022.17058
- Pastor, M., Blanc, T., Haddad, B., Petrone, S., Sanchez Morles, M., Drempetic, V., Issler, D., Crosta, G. B., Cascini, L., Sorbino, G., & Cuomo, S. (2014). Application of a SPH depth-integrated model to landslide run-out analysis. *Landslides*, 11(5), 793–812. https://doi.org/10.1007/s10346-014-0484-y
- Pirulli, M., & Sorbino, G. (2008). Assessing potential debris flow runout: a comparison of two simulation models. *Natural Hazards and Earth System Sciences*, 8(4), 961–971. https://doi.org/10.5194/nhess-8-961-2008
- Pitman, E. B., Nichita, C. C., Patra, A., Bauer, A., Sheridan, M., & Bursik, M. (2003). Computing granular avalanches and landslides. *Physics of Fluids*, 15(12), 3638–3646. https://doi.org/https://doi.org/10.1063/1.1614253
- Ruiz-Villanueva, V., Bladé, E., Sánchez-Juny, M., Marti-Cardona, B., Díez-Herrero, A., & Bodoque, J. M. (2014). Two-dimensional numerical modeling of wood transport. *Journal of Hydroinformatics*, 16(5), 1077. https://doi.org/10.2166/hydro.2014.026
- Ruiz-Villanueva, V., Mazzorana, B., Bladé, E., Bürkli, L., Iribarren-Anacona,

- P., Mao, L., Nakamura, F., Ravazzolo, D., Rickenmann, D., Sanz-Ramos, M., Stoffel, M., & Wohl, E. (2019). Characterization of wood-laden flows in rivers. *Earth Surface Processes and Landforms*, 44(9), 1694–1709. https://doi.org/10.1002/esp.4603
- Sanz-Ramos, M., Téllez-Álvarez, J., Bladé, E., & Gómez-Valentín, M. (2019). Simulating the hydrodynamics of sewer-grates using a 2D-hydraulic model. 5th International Conference SimHydro, 8.
- Sanz-Ramos, M., Martí-Cardona, B., Bladé, E., Seco, I., Amengual, A., Roux, H., & Romero, R. (2020). NRCS-CN Estimation from Onsite and Remote Sensing Data for Management of a Reservoir in the Eastern Pyrenees. *Journal of Hydrologic Engineering*, 25(9), 05020022. https://doi.org/10.1061/(ASCE)HE.1943-5584.0001979
- Sanz-Ramos, M., Andrade, C. A., Oller, P., Furdada, G., Bladé, E., & Martínez-Gomariz, E. (2021). Reconstructing the Snow Avalanche of Coll de Pal 2018 (SE Pyrenees). GeoHazards, 2(3), 196–211. https://doi.org/10.3390/geohazards2030011
- Sanz-Ramos, M., Olivares, G., & Bladé, E. (2022). Experimental characterization and two-dimensional hydraulic-hydrologic modelling of the infiltration process through permeable pavements. Revista Internacional de Métodos Numéricos Para Cálculo y Diseño En Ingeniería, 38(1). https://doi.org/10.23967/j.rimni.2022.03.012
- Sanz-Ramos, M., Bladé, E., Oller, P., & Furdada, G. (2023a). Numerical modelling of dense snow avalanches with a well-balanced scheme based on the 2D shallow water equations. *Journal of Glaciology*, 1–17. https:// doi.org/10.1017/jog.2023.48
- Sanz-Ramos, M., Bladé, E., & Sánchez-Juny, M. (2023b). El rol de los términos de fricción y cohesión en la modelización bidimensional de fluidos no Newtonianos: avalanchas de nieve densa. *Ingeniería Del Agua*, 27(4), 295–310. https://doi.org/10.4995/ia.2023.20080
- Sanz-Ramos, M., López-Gómez, D., Bladé, E., & Dehghan-Souraki, D. (2023c). A CUDA Fortran GPU-parallelised hydrodynamic tool for high-resolution and long-term eco-hydraulic modelling. *Environmental Modelling & Software*, 161(ii), 105628. https://doi.org/10.1016/j. envsoft.2023.105628
- Sanz-Ramos, M., Bladé, E., Sánchez-Juny, M., & Dysarz, T. (2024a). Extension of Iber for Simulating Non–Newtonian Shallow Flows: Mine-Tailings Spill Propagation Modelling. Water, 16(14), 2039. https://doi.org/10.3390/w16142039
- Sanz-Ramos, M., Bladé, E., Silva-Cancino, N., & Salazar, F. (2024b). Avances en Iber para la clasificación de balsas: proyecto ACROPOLIS. *Ingeniería Del Agua*, 28(1), 47–63. https://doi.org/10.4995/ia.2024.20609
- Sanz-Ramos, M., Vales-Bravo, J. J., Bladé, E., & Sánchez-Juny, M. (2024c). Reconstructing the spill propagation of the Aznalcóllar mine disaster. Mine Water and the Environment, 43(3). https://doi.org/10.1007/ s10230-024-01000-5
- Sanz-Ramos, M., Sañudo, E., López-Gómez, D., García-Feal, O., Bladé, E., & Cea, L. (2025). Evolución de la modelización numérica bidimensional del flujo en lámina libre a través del software Iber. *Ingeniería Del Agua*, 29(2), 114–131. https://doi.org/10.4995/ia.2025.23259

- Satria, H., Nurfaida, W., Kurniawan, A., Iswardoyo, J., & Sulaiman, M. (2024). Numerical simulation and redesign of Kamar Kajang Levee against Mount Semeru lahar flood based on HEC-RAS 2D non-newtonian flow model. *IOP Conference Series: Earth and Environmental Science*, 1311(1), 12065. https://doi.org/10.1088/1755-1315/1311/1/012065
- Schilling, S. P. (2014). Laharz\_py: GIS tools for automated mapping of lahar inundation hazard zones. (Open-File Report 2014-1073) United States Geological Survey. https://doi.org/10.3133/ofr20141073
- Schraml, K., Thomschitz, B., McArdell, B. W., Graf, C., & Kaitna, R. (2015). Modeling debris-flow runout patterns on two alpine fans with different dynamic simulation models. *Natural Hazards and Earth System Sciences*, 15(7), 1483–1492. https://doi.org/10.5194/nhess-15-1483-2015
- Sheridan, M. F., Hubbard, B., Carrasco-Núñez, G., & Siebe, C. (2004). Pyroclastic flow hazard at volcán Citlaltépetl. *Natural Hazards*, 33(2), 209–221. https://doi.org/10.1023/B:NHAZ.0000037028.89829.d1
- Syarifuddin, M., Oishi, S., Hapsari, R. I., & Legono, D. (2018). Empirical model for remote monitoring of rain-triggered lahar at Mount Merapi. *Journal* of *Japan Society of Civil Engineers, Ser. B1 (Hydraulic Engineering)*, 74(4), I\_1483-I\_1488. https://doi.org/10.2208/jscejhe.74.I\_1483
- Thouret, J. C., Antoine, S., Magill, C., & Ollier, C. (2020). Lahars and debris flows: Characteristics and impacts. *Earth-Science Reviews*, 201, 103003. https://doi.org/10.1016/j.earscirev.2019.103003
- Tierz, P., Woodhouse, M. J., Phillips, J. C., Sandri, L., Selva, J., Marzocchi, W., & Odbert, H. M. (2017). A Framework for Probabilistic Multi-Hazard Assessment of Rain-Triggered Lahars Using Bayesian Belief Networks. Frontiers in Earth Science, 5. https://doi.org/10.3389/feart.2017.00073
- Vera, P., Ortega, P., Casa, E., Santamaría, J., & Hidalgo, X. (2019). Modelación Numérica y Mapas de Afectación por Flujo de Lahares Primarios en el Drenaje Sur del Volcán Cotopaxi. Revista Politécnica, 43(1), 61–72. https://doi.org/10.33333/rp.vol43n1.971
- Vignaux, M., & Weir, G. J. (1990). A general model for Mt. Ruapehu lahars. Bulletin of Volcanology, 52(5), 381–390. https://doi.org/10.1007/ BF00302050
- Voellmy, A. (1955). Über die Zerstörungskraft von Lawinen. Schweizerische Bauzeitung, 73, 15. https://doi.org/10.5169/seals-61891
- Woodhouse, M. J., Johnson, C. G., Hogg, A. J., Phillips, J. C., Espin Bedon, P., Almeida, S., & Andrade, S. D. (2016). A model of lahars for hazard assessment. 90 Conference Cities on Volcanoes, Puerto Varas, Chile, November 20-25, 2016.